Chapter 1

Results

For all values of the control parameter,B, we observed that the nearest neighbour distributions deviate from both the Poisson and Wigner distributions. We propose the following hypothesis: the obtained nearest neighbour distributions can be seen as a linear superposition of the Poisson and Wigner distributions:

$$P(s) = \alpha P_P(s) + (1 - \alpha) P_W(s).$$

This hypothesis is rooted in the fact that the classical counterpart of our system has an interplay between regular and chaotic motion clearly illustrated by the Poincaré sections in figures 1.1 [1]. In this way we consider that for a range of energies of the classical system, the phase space ratio of the volumes of chaotic and regular trajectories is reflected in the the superposition of Wigner and Poisson distributions.

Thus, a system with an integrable classical counterpart will have $\alpha = 1$, corresponding to the Poisson distribution, while a fully chaotic system will have $\alpha = 0$ corresponding to the Wigner distribution. For a system which has balanced contributions to the phase space volume both from the regular and chaotic trajectories, we expect the Poisson and Wigner distributions to equally contribute to $P(s)$.

For the fixed value of the non-integrability parameter of $B = 0.55$ we observe that with the increase of energy, the phase space fills with tori up to a energy of around $E = 600$ (in units of harmonic oscillator energy) and after that the chaotic trajectories begin to fill the phase space. We can say that globally, for an energy range $\Delta E \leq 600$, the phase space is characterised by an increase of regular trajectories as the energy increases. If we now consider the quantum counterpart of the system, we can use α as a measure of the closeness to the Poisson distribution. As we can see in figures 1.2 and 1.3 with the increase of the energy interval α increases from 0.493 at $\Delta E \approx 100$ to 0.876 at $\Delta E \approx 180$.

Thus, at least for a fixed value of B, we can observe a correlation between the tori volume in phase space and α, the superposition coefficient.

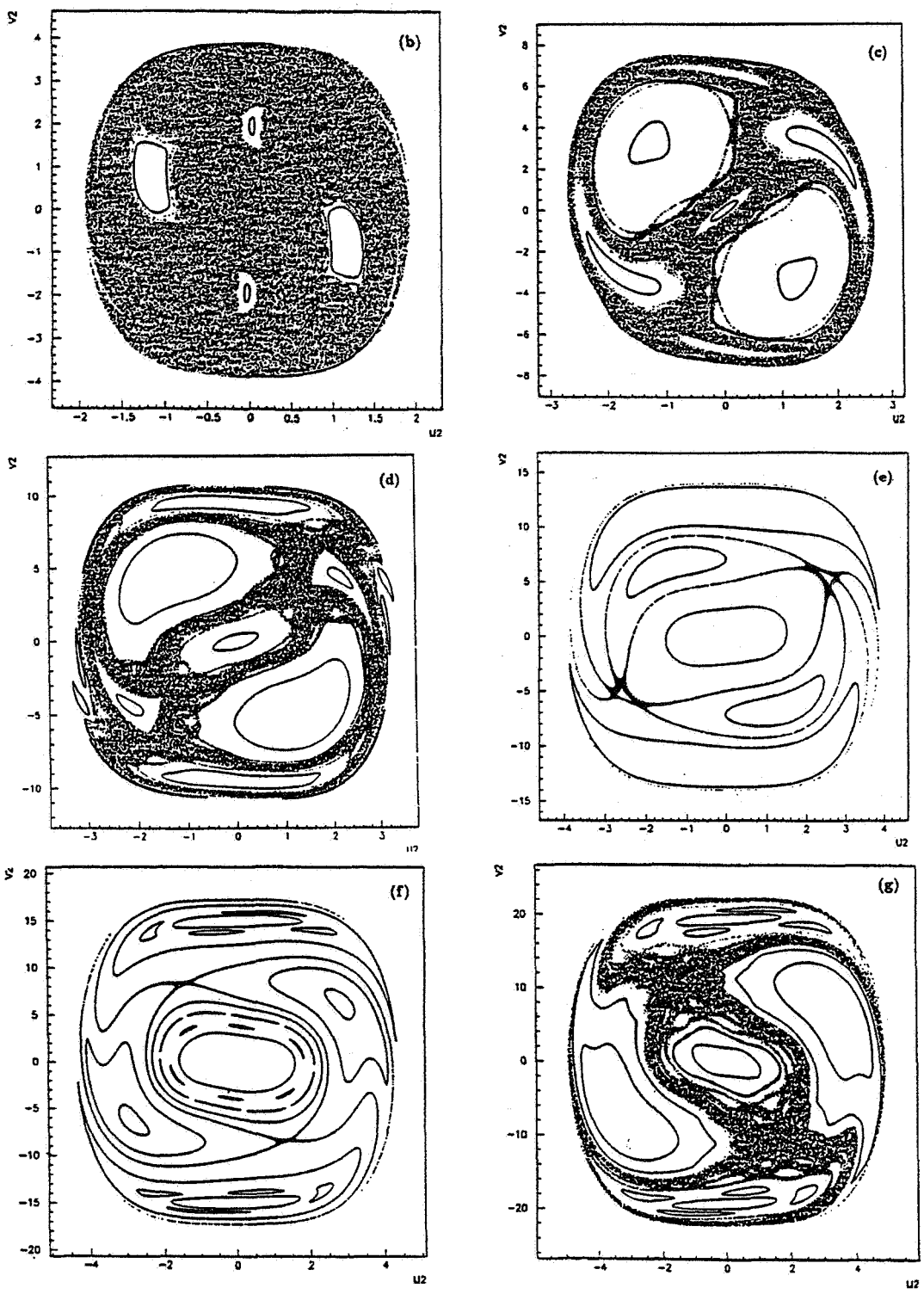

Figure 1.1: Poincaré sections for $B = 0.55$ and $E = 30A$(MeV) (b), $E = 120A$(MeV) (c), $E = 240A$(MeV) (d), $E = 400A$(MeV) (e), $E = 600A$(MeV) (f), $E = 1000A$(MeV) (g).

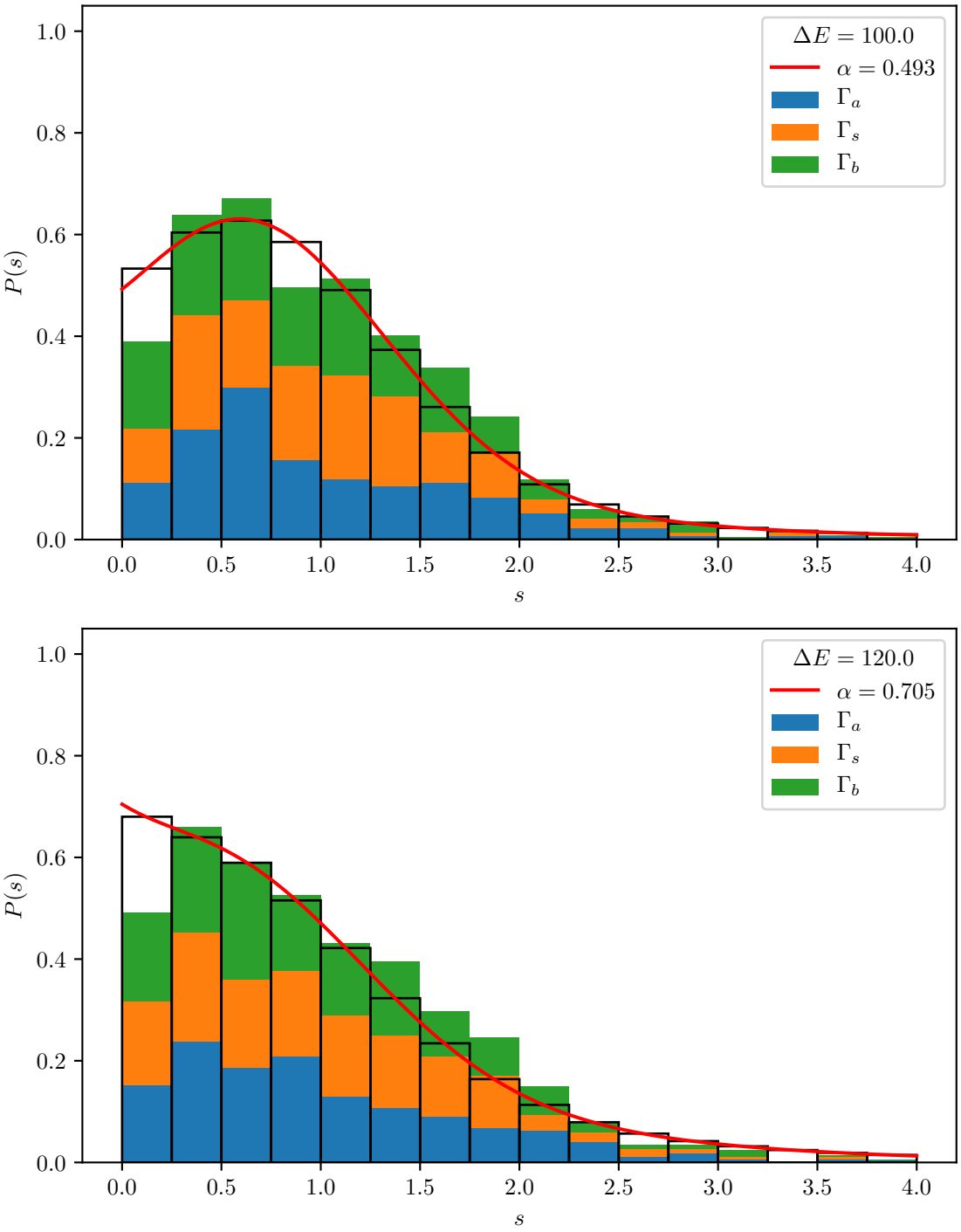

Figure 1.2: $P(s)$ for $B = 0.55, D = 0.4, N = 260$ and $\Delta E_{max} = 100, 120$

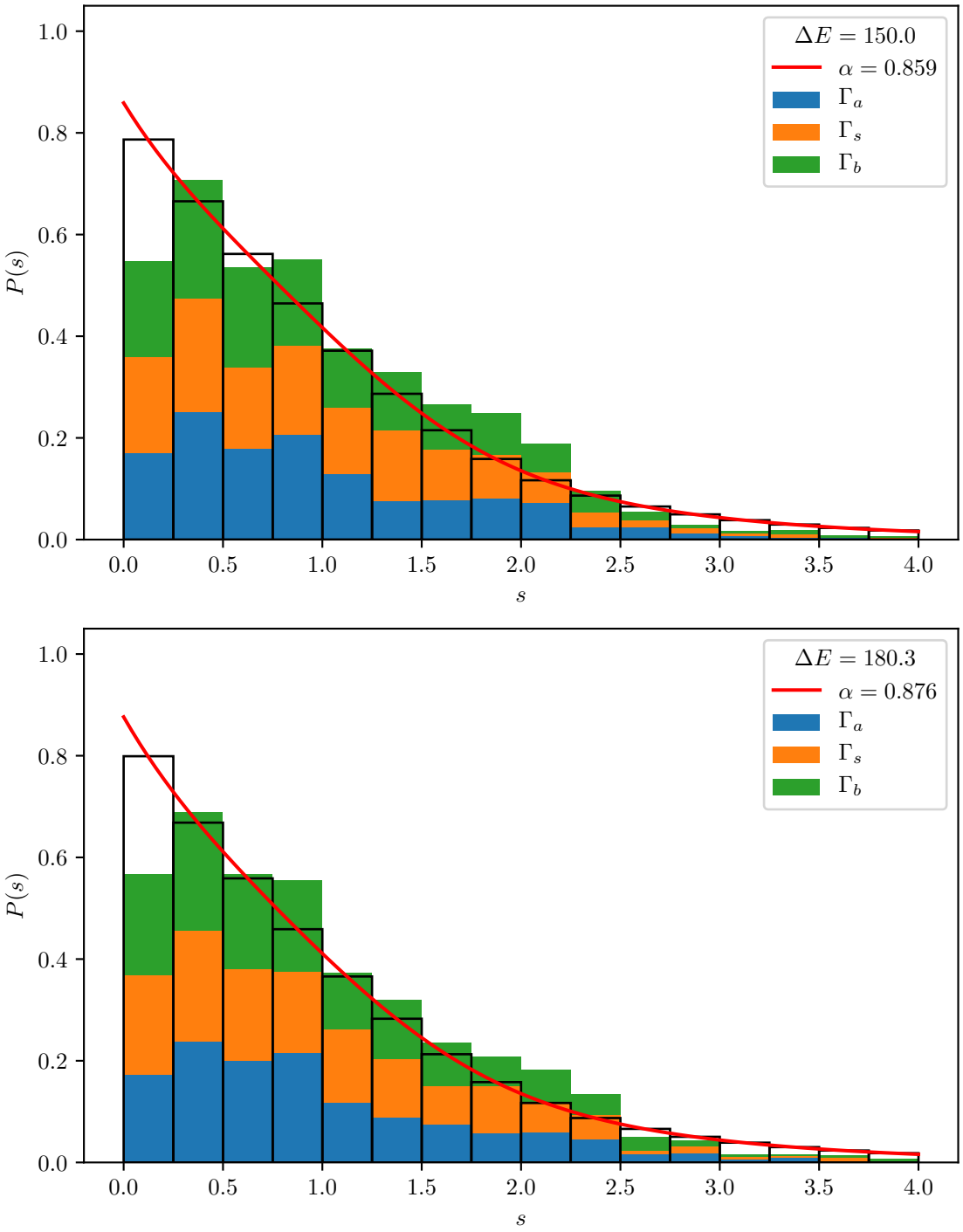

Figure 1.3: $P(s)$ for $B = 0.55, D = 0.4, N = 260$ and $\Delta E_{max} = 150, 180.3$

Looking at other values for B such as $B = 0.2$ and $B = 0.63$, we observe that $P(s)$ gets closer to a Poisson distribution with the increase of energy (see figs. 1.4 to 1.7). This global feature of the system can be observed on the entire interval from $B = 0.01$ to $B = 0.63$. In order to emphasise this, we plot α as a function of ΔE (see figs. 1.8 to 1.11).

This remarkable behaviour can be viewed as consequence of the interplay of the third and fourth order terms in the Hamiltonian. The third order terms, which consist in the non-integrable part of the Hamiltonian and can be considered as contributing to the apparition of chaotic trajectories.

An other global characteristic of the system can be revealed by studying the dependence of α on the non-integrability parameter B. In figure 1.12 $\alpha(B)$ is plotted for different values of N. The value of N determines both the stability of the values and the maximum energy interval. Indeed, since our method implies the truncation of the Hilbert space, we restrict the number of considered energy levels with the stability criterion.

As with the above case of $\alpha(\Delta E)$, we can reduce the energy interval by considering only the energy levels up to a given value. In figures 1.13 and 1.14 we can see that the shape of $\alpha(B)$ for $N = 260$ remains qualitatively the same when we consider different values for the maximum energy interval. We can observe that as we increase the energy the values of α globally rise, as expected from the previous plots.

An other qualitative test of our data implies checking how the values of α change when we consider different values for N, in this case $N = 220, 240, 260$ and different energy intervals. By considering multiple values for N we can check the stability of the energy levels within a given interval provided that the respective interval is less than the maximum energy interval for all N. In figs. 1.15 to 1.17 we can see that indeed the energy levels are stable as the values of α barely change.

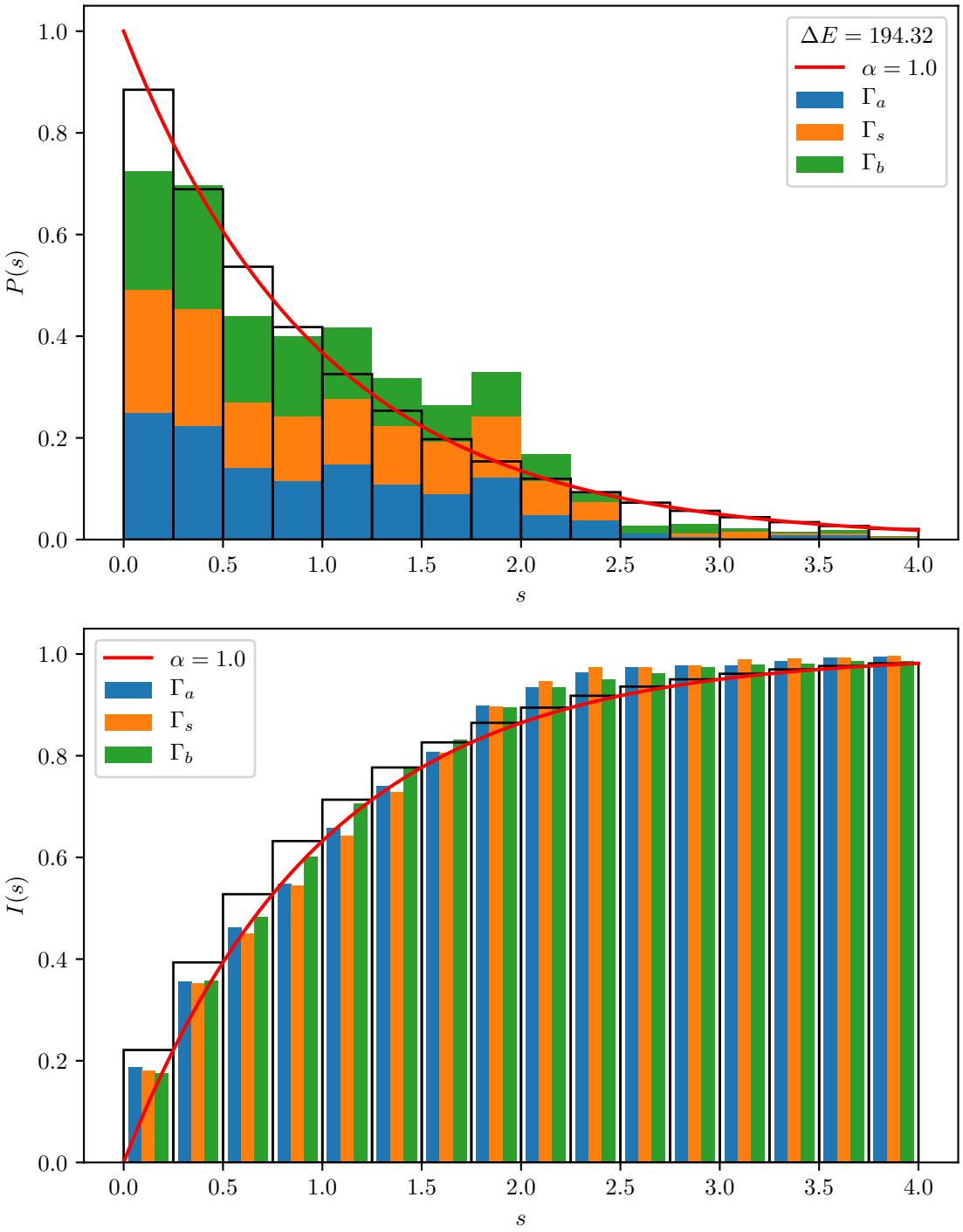

Figure 1.4: $P(s), I(s)$ for $B = 0.2, D = 0.4, N = 260$

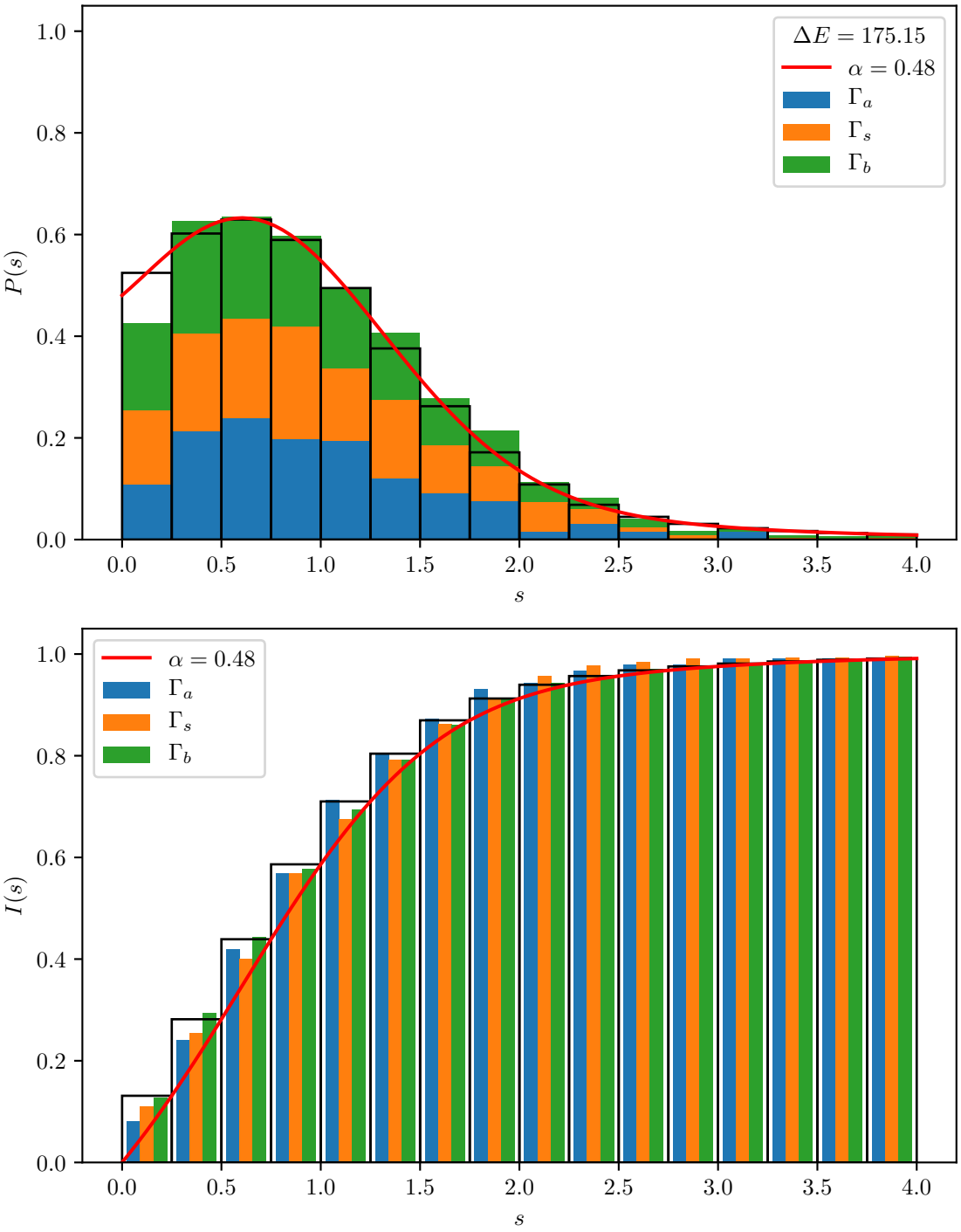

Figure 1.5: $P(s), I(s)$ for $B = 0.63, D = 0.4, N = 260$

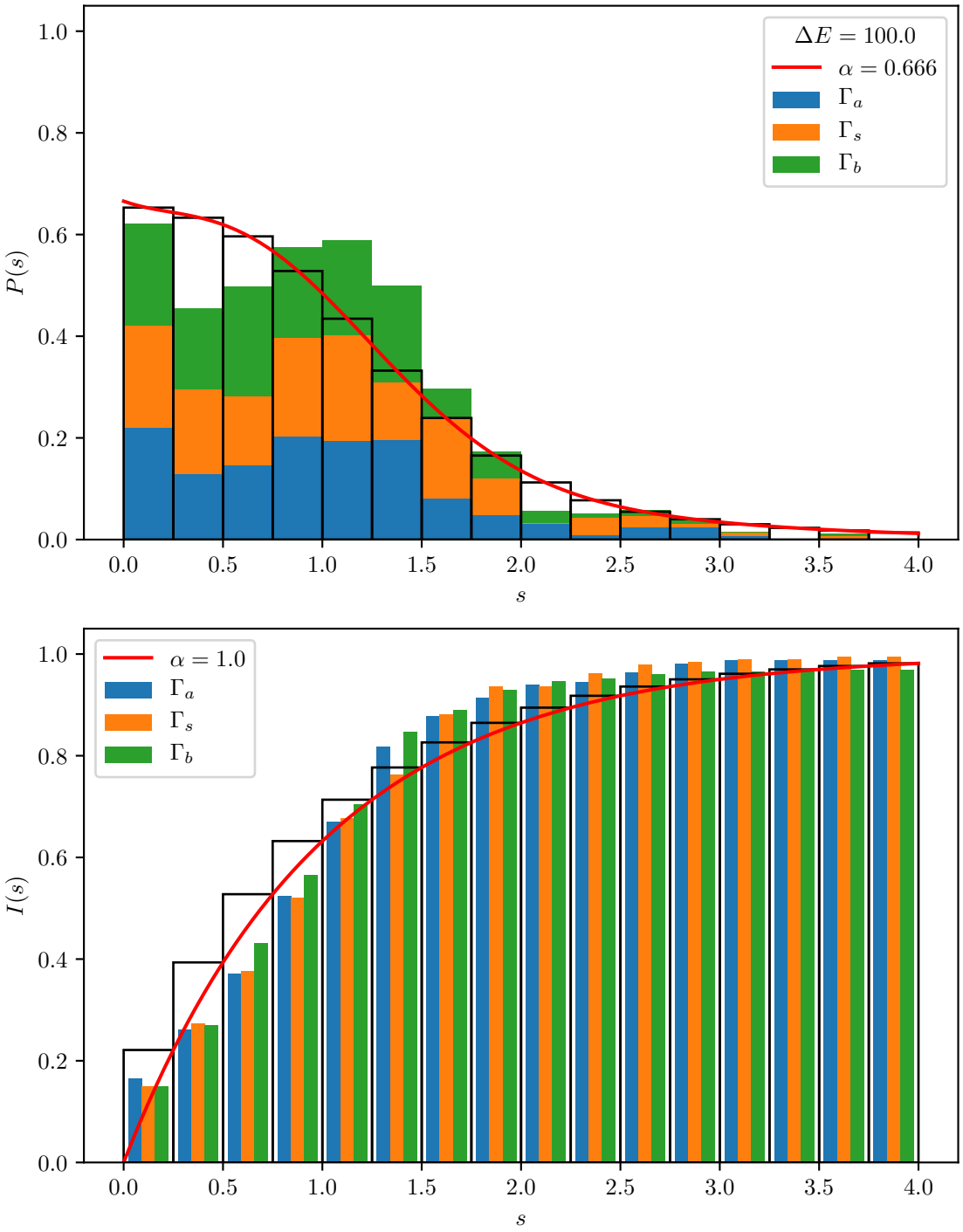

Figure 1.6: $B = 0.2, D = 0.4, N = 260, \Delta E_{max} = 100$

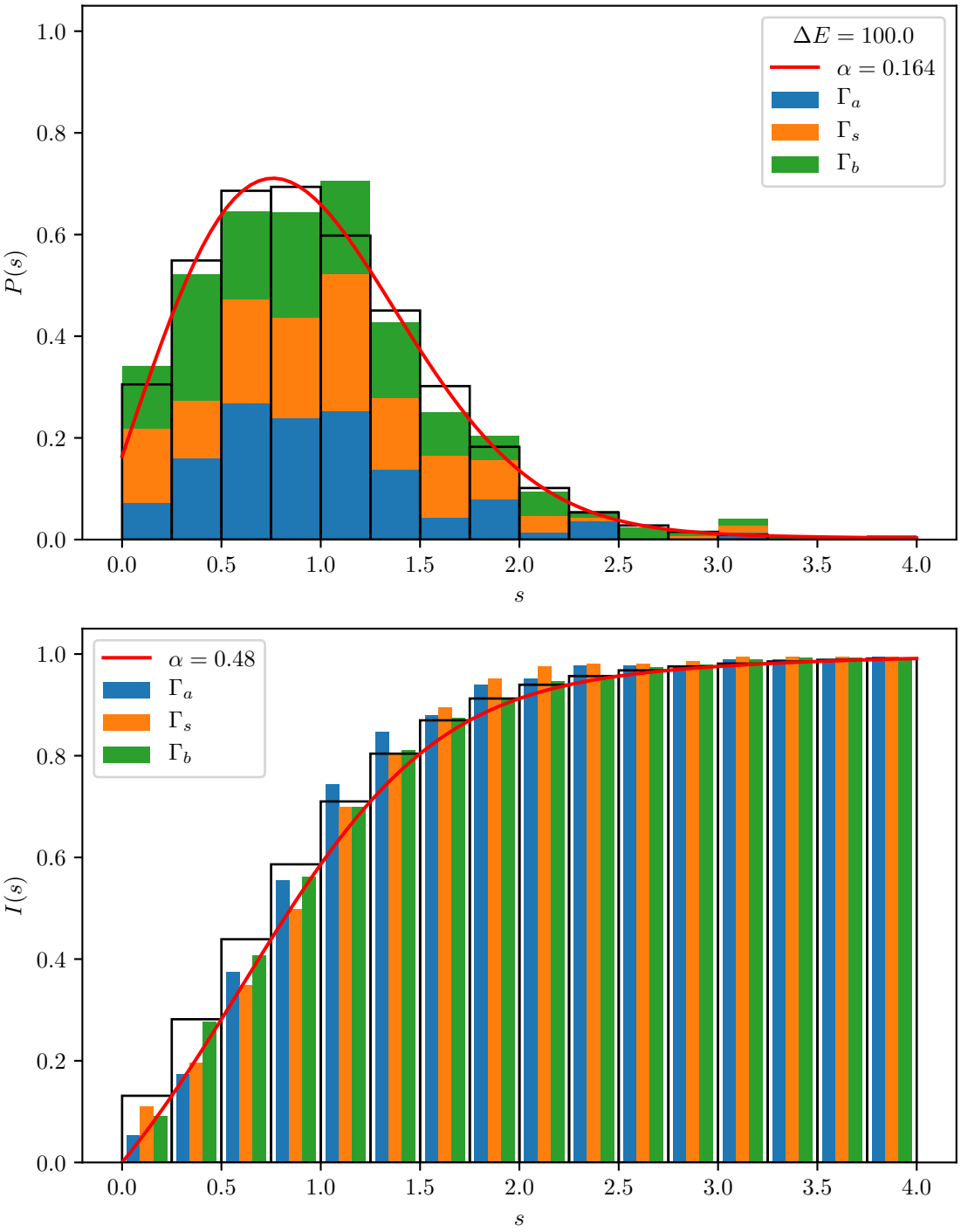

Figure 1.7: $B = 0.63, D = 0.4, N = 260, \Delta E_{max} = 100$

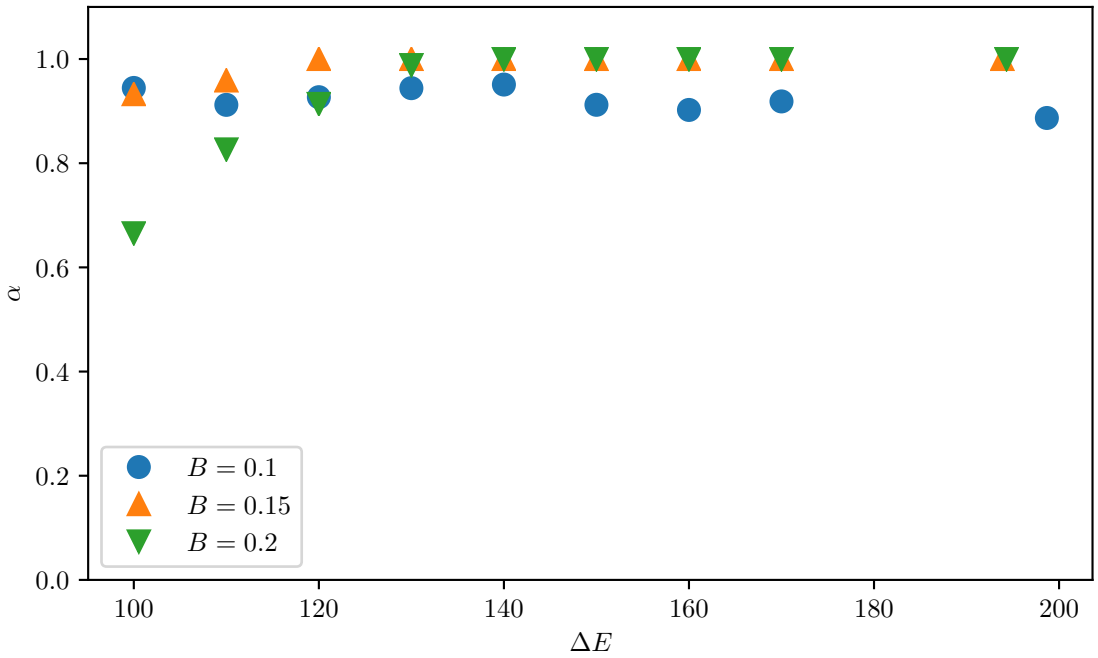

Figure 1.8: $B = 0.1, 0.15, 0.2,\ N = 260$

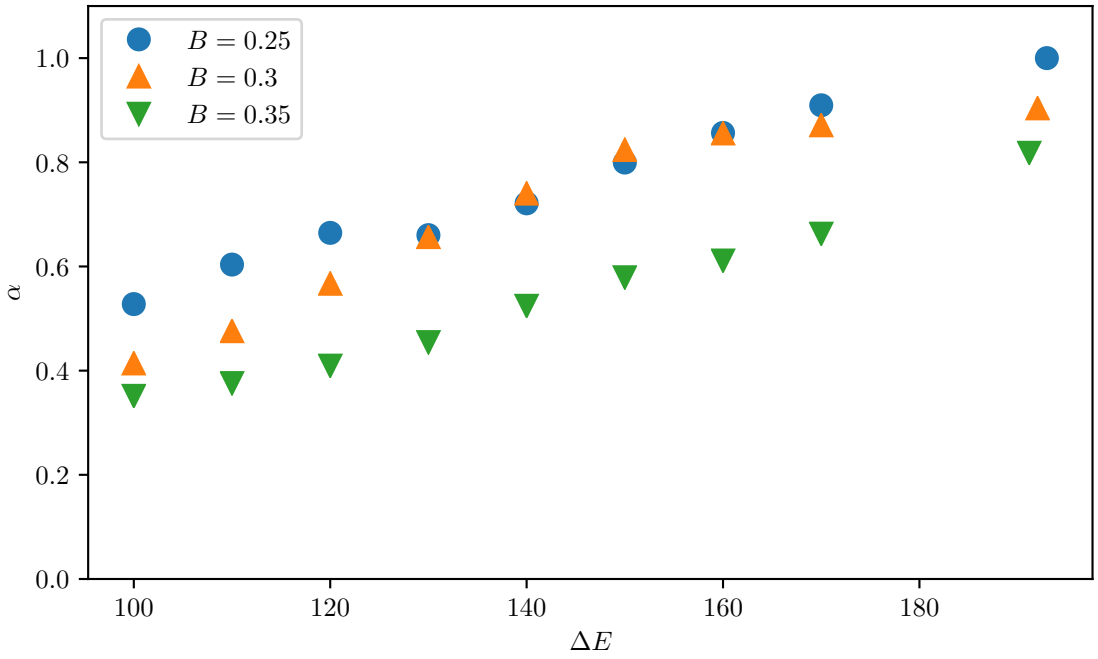

Figure 1.9: $B = 0.25, 0.3, 0.35,\ N = 260$

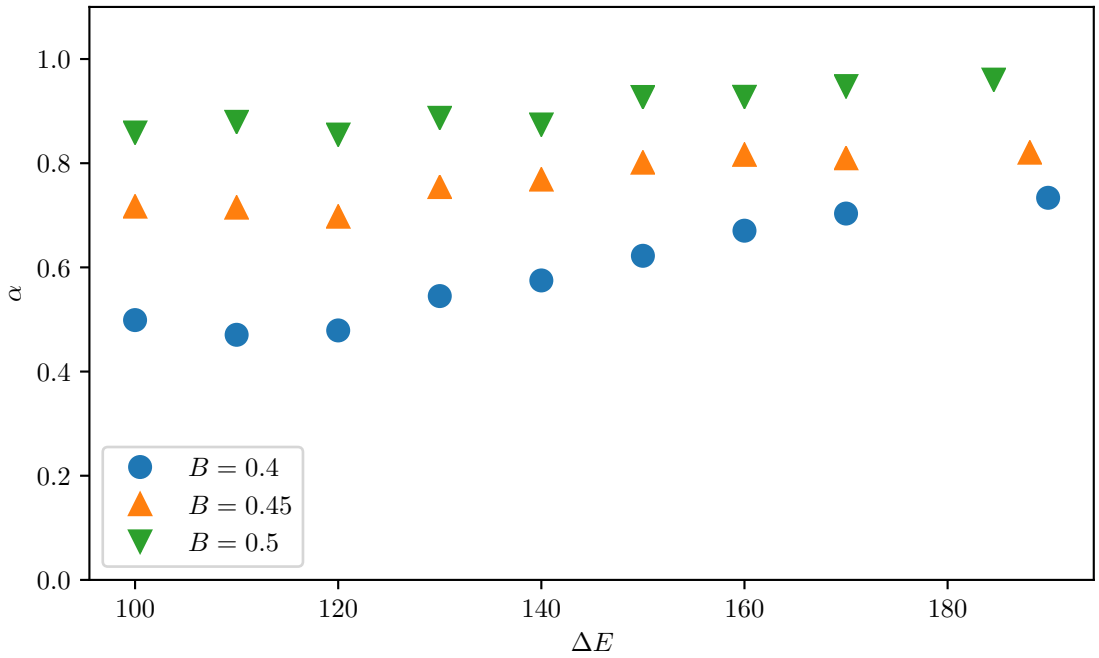

Figure 1.10: $B = 0.4, 0.45, 0.5,\ N = 260$

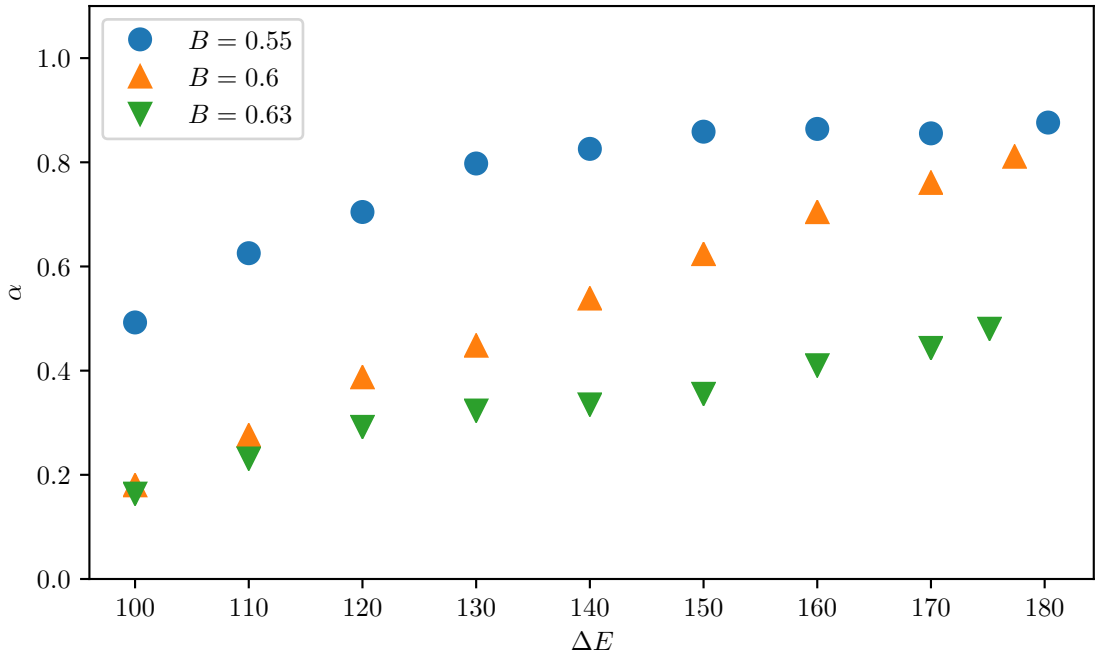

Figure 1.11: $B = 0.55, 0.6, 0.63,\ N = 260$

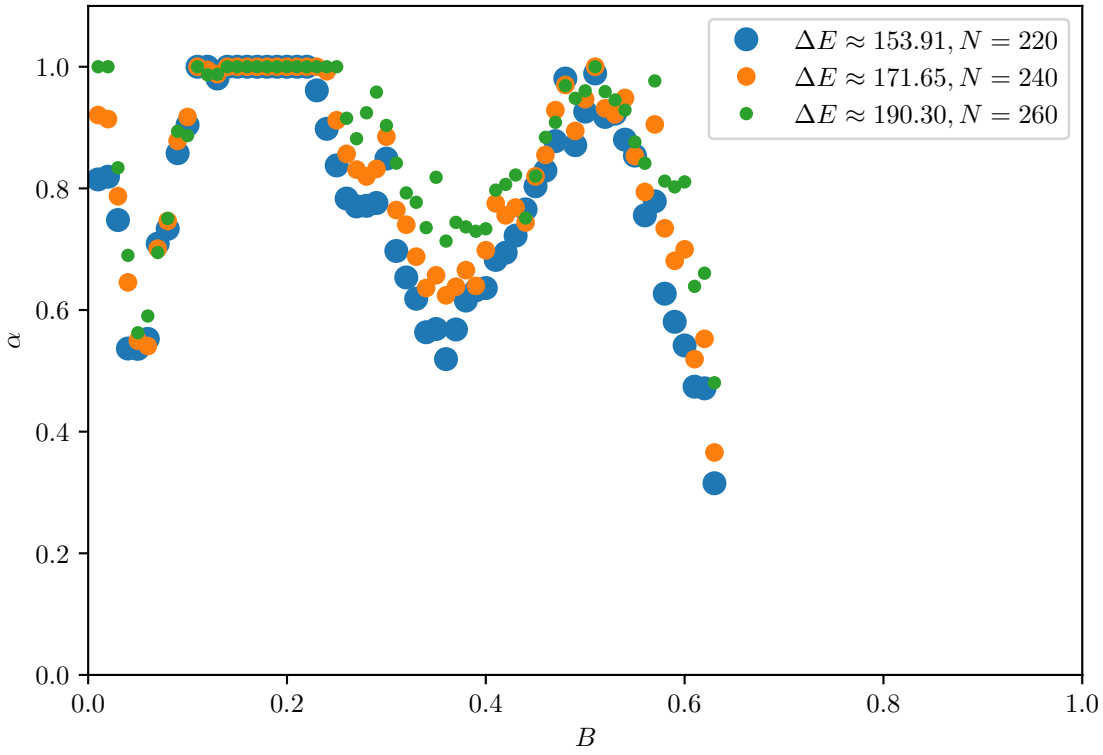

Figure 1.12: $N = 220, 240, 260$

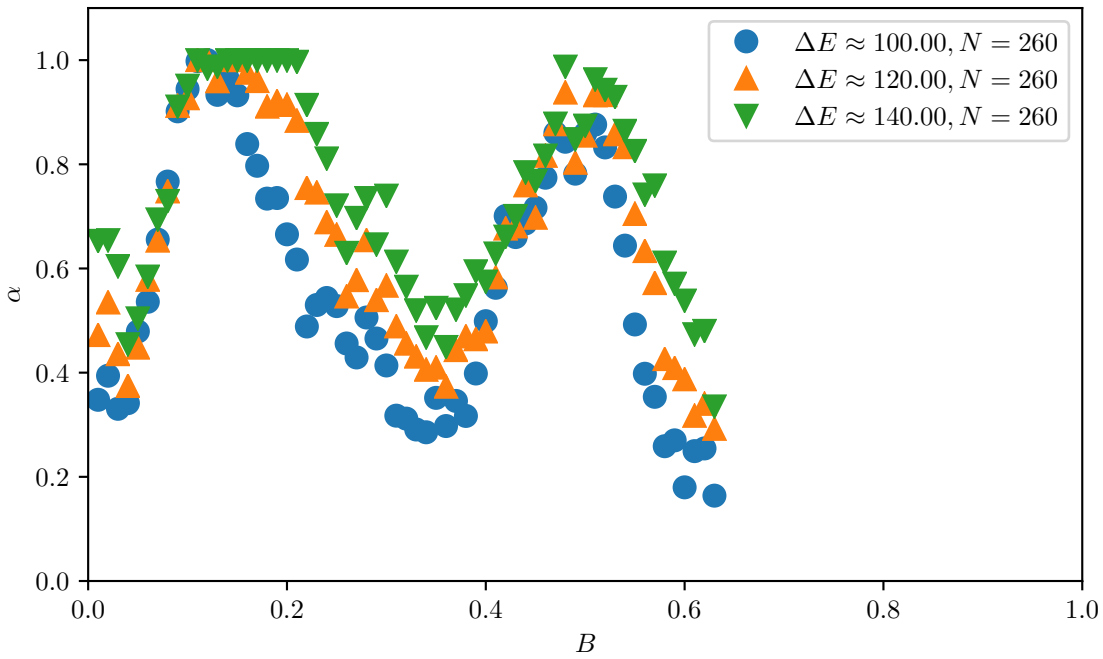

Figure 1.13: $N = 260,\ \Delta E_{max} \approx 100, 120, 140$

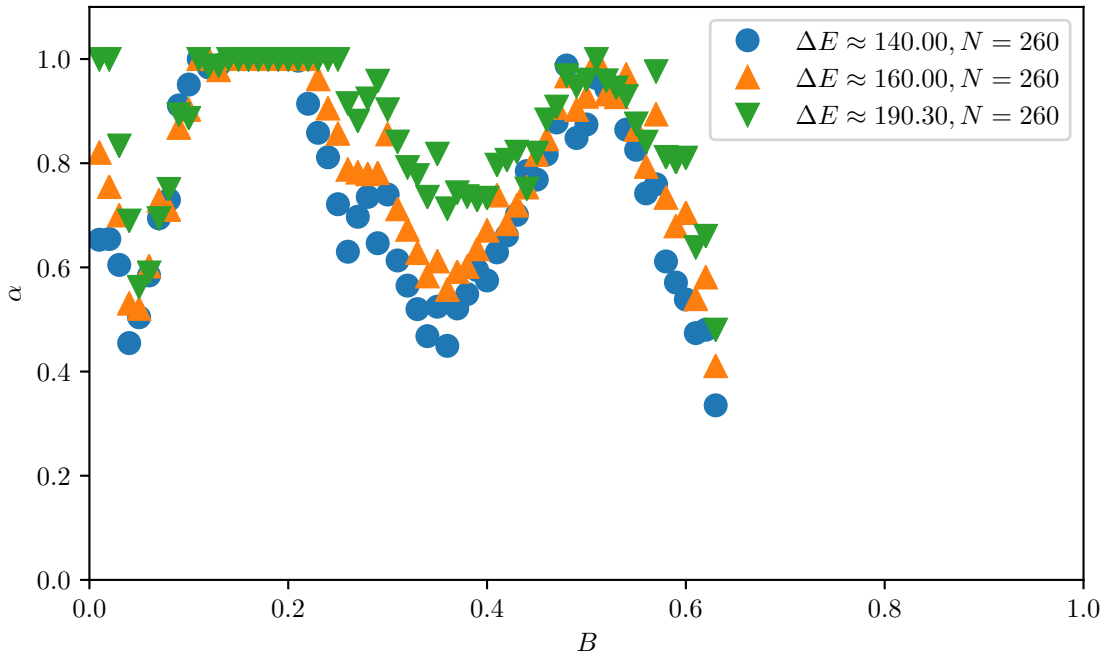

Figure 1.14: $N = 260,\ \Delta E_{max} \approx 140, 160, 190.305$

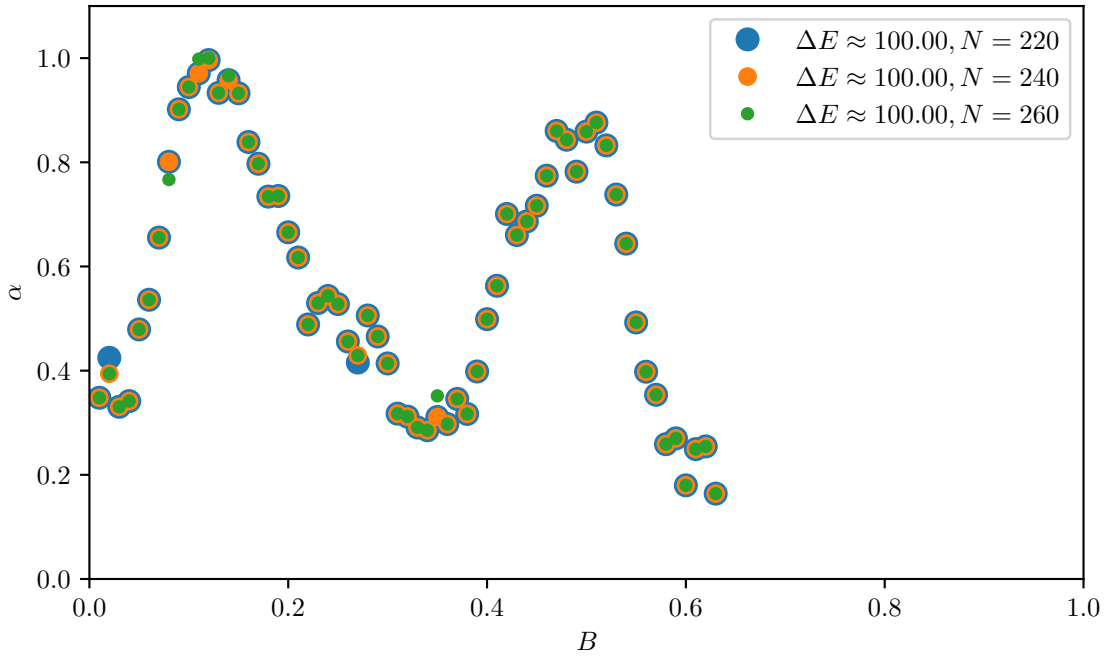

Figure 1.15: $N = 220, 240, 260,\ \Delta E_{max} \approx 100$

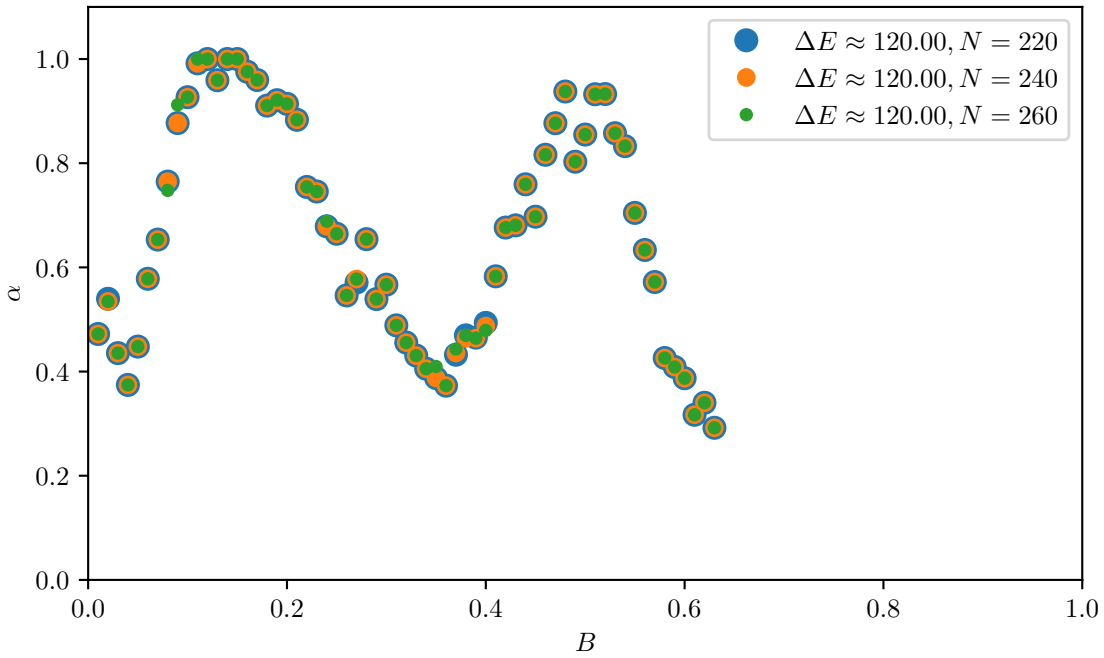

Figure 1.16: $N = 220, 240, 260,\ \Delta E_{max} \approx 120$

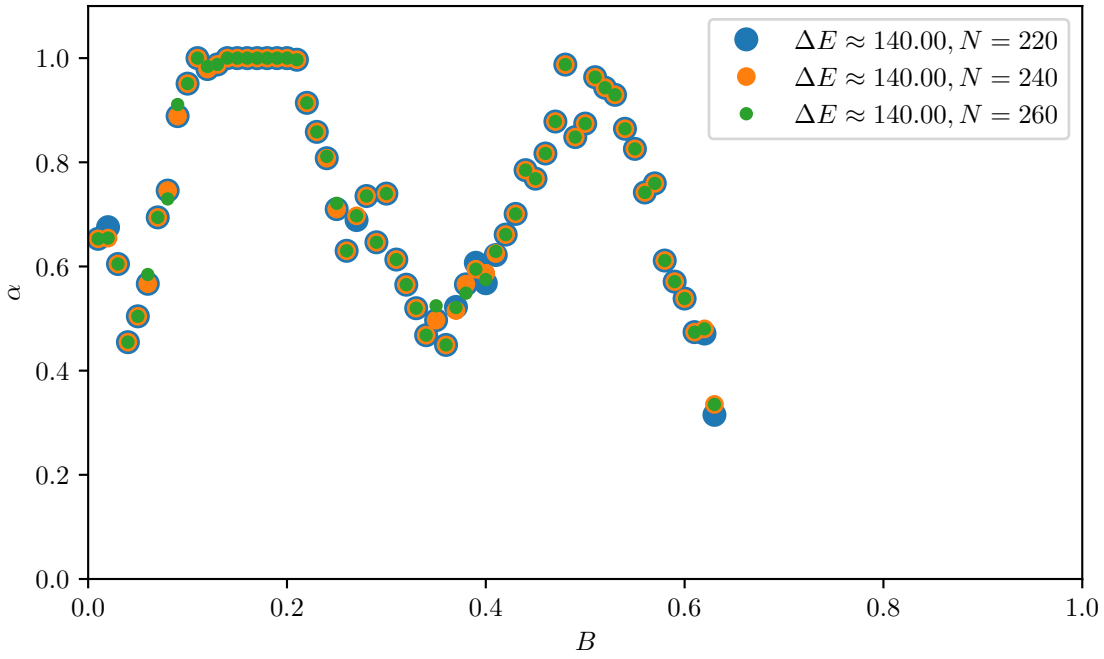

Figure 1.17: $N = 220, 240, 260,\ \Delta E_{max} \approx 140$